This is the accepted version of the following article: , Kennedy, M., Ahmed, H., Doran, J., Norton, B., Bosch-Jimenez, P., Pirriera, M. D., Torralba-Calleja, E., Tauste, D. G., Aubouy, L., Daren, S., Solomon-Tsvetkov, F., Galindo, S., Voz, C. and Puigdollers, J. (2015), **Large Stokes shift downshifting Eu(III) films as efficiency enhancing UV blocking layers for dye sensitized solar cells**. Phys. Status Solidi A, 212: 203–210. doi: 10.1002/pssa.201431683 , *which has been published in final form at http://onlinelibrary.wiley.com/doi/10.1002/pssa.201431683/epdf*

Large Stokes Shift Downshifting Organolanthanide Films as Efficiency-Enhancing ultra-violet Blocking-Layers for dye-sensitised solar cells.

M. Kennedy[a], H. Ahmed[a], J. Doran[a], B. Norton[a], P.Bosch Gimenez[b], M. Della Pirriera[b], D. Gutiérrez Tauste[b], S. Daren[c], F. Solomon-Tsvetkov[c], S. Galindo[d], C. Voz[d], J. Puigdollers[d]

[a] Dublin Energy Lab, Dublin Institute of Technology, Kevin St., Dublin 8, Ireland.
[b] Leitat Technological Center, C/ de la Innovació, 2 , Terrassa 08225, Spain.
[c] Daren Laboratories, 13 Hamazmera street, Ness-Ziona, 74047, Israel.
[d] Universitat Politècnica Catalunya, C/Jordi Girona, 31, Mòdul C4, Barcelona 08034, Spain

Abstract

In dye-sensitised solar cells developed to-date, ultraviolet blocking layers (UV-BL) is employed to avoid photocatalysis effects on the dye and consequent reduction in PV energy output over time due to UV exposure in outdoor conditions. Use of a UV-BL increases stability but, power conversion efficiency decreases as incident UV photons are not converted. The organolanthanide complex $Eu(tta)_3phen$ is examined for inclusion in large Stokes shift downshifting (LSS DS) layers. It is shown that such LSS DS layers can be used as a UV blocking layer in DSSCs. A ray-trace numerical model is used to optimise the thickness and concentration of the LSS DS layers for the specific N719 DSSC. EQE is significantly increased in the UV spectral region compared to DSSCs utilizing a passive, non-luminescent, UV-BL. High $Eu(tta)_3phen$ film transparency in the visible range minimises DSSC EQE losses at visible wavelengths. The photostability of the blended LSS DS polymer films is not sufficient to be useful for medium-long term outdoor PV applications. However, the results demonstrate that significant efficiency enhancement can be realized. Short circuit current enhancement due to downshifting is demonstrated (~1%) in small scale LSS DS polymer films prepared and attached to DSSC devices, where the specific geometry limits the photon collection efficiency and overall enhancement. Model predictions indicate that 2-3% enhancement is realizable in DSSC minimodules, compared to minimodules using passive, non-luminescent, UV-BL. Predicted enhancement in *energy* produced in outdoor conditions is 3-5%.

1. Introduction

A major part of the existing photovoltaic (PV) market comprises inorganic semiconductor solar modules that require high costs and high energy consuming fabrication processes and, in some cases, the use toxic materials (such as Cadmium in as Cadmium Telluride based PV). Organic Dye Sensitized Solar Cells [1, 2] (DSSC) can use low temperature, low cost fabrication processes and primarily organic materials in production. DSSC have attained comparable efficiencies to inorganic amorphous silicon PV with efficiencies in small DSSC (active area ~1 cm^2) of approximately 11%, and in submodules (active area ~17 cm^2) of 9.9% [3]. Research to improve the DSSC cell stability, would allow more widespread uptake. Light soaking tests over 1000 hours at 60ºC on a 0.158 cm^2 DSSC, gave a 5% reduction of initial efficiency [4]. Kato et al. have exposed DSSC under 15000 hours light soaking at 60ºC, and estimate a lifetime of approximately 15 years [5]. In the case of larger DSSC modules (110 cm^2) tested over a 6 month period, the extrapolated lifetime performance reduction is 6% per year. In DSSC ageing tests, ultraviolet blocking layers (UV-BL) are used to avoid photocatalysis effects on the dye and consequent reduction in energy output over time [4, 6]. While the use of UV-BL increases stability compared to a bare DSSC, the power conversion efficiency of the DSSC decreases as the incident UV photons remain unconverted. The paper shows how large Stokes shift downshifting (LSS DS) layers can be used as a "active" UV blocking layer that also enhances efficiency relative to DSSCs utilizing "passive", non-luminescent UV-BL.

Luminescent DS layers [7] can enhance the short circuit current (Isc) of PV cells by transforming the wavelength of incident light from short to longer wavelengths thus better matching the spectral response of the cell. Luminescent materials have been researched for PV applications

[8,9] include organic dyes [10], inorganic semiconductor nanocrystals [11], and lanthanide complexes [12, 13]. Prototype devices have been developed incorporating DS layers applied to inorganic semiconductor solar cells [10,14,15, 16, 17, 18]. In the case of DSSC DS applications, Slooff et al. [19] investigation of various DS organic dyes in polymeric host materials found Isc enhancement was observed, primarily due to unwanted dye absorption in the visible range (i.e. overlap between the dyes' absorption spectra and the DSSC external quantum efficiency, EQE). In this study, UV-absorbing DS materials exhibiting large Stokes shifted photoluminescence (PL) are utilized, thereby minimising transmission losses at visible wavelengths. Slooff et al. [19] also discuss how optical losses arising from the specific geometry of the DSSC could limit measured DS gains. In this study, ray-trace modelling is employed to show how these optical losses can be reduced in prototype single-cell DS/DSSC devices. Liu et al. [20] showed how externally applied $LaVO_4$:Dy LSS DS nanocrystals can act as a UV blocker resulting in increased DSSC stability, however efficiency enhancement was observed relative to the bare DSSC, and no comparison was made with DSSC incorporating a passive, non-luminescent UV-BL layer as is presented here. In addition, this study presents luminescent quantum yield measurements of the solid LSS DS films. Another approach reported in the literature is to introduce the DS material into the *internal* DSSC architecture. TiO_2 doping with $Gd_2O_3:Sm^{3+}$ luminescent nanoparticles, has demonstrated large enhancement in efficiency (12.6 % increase relative to device with no nanoparticles) [21]. The enhancement due to spectrum modification through *downshifting*, and the enhancement due to more optimal doping is not quantified, however. In this paper, externally applied DS layers were employed and the enhancement quantified was qualified using spectrally-resolved EQE characterisation.

The organolanthanide complex $Eu(tta)_3phen$ has been examined for inclusion in LSS DS layers acting as externally applied UV blocking layers for DSSCs. The Europium based complex absorbs in the UV region and exhibits photoluminescence (PL) at "red" wavelengths. Polymer films are prepared and "N719" type DSSC devices were fabricated as described in section 2. A ray-trace numerical model of PV/DS devices presented in section 3, was used to optimise the thickness and concentration of the LSS DS layers for the specific DSSC. The PL and stability properties of the LSS DS films evaluations are discussed in section 4. The 390 nm cutoff cut-off wavelength of the $Eu(tta)_3phen$ film is analogous to passive UV-BL typically used in DSSCs. It is shown that a high visible transparency in the visible range of the *LSS* DS $Eu(tta)_3phen$ films results in no significant EQE losses at visible wavelengths. Short circuit current enhancement due to downshifting is demonstrated (~1%) in small scale DSSC prototypes, for which the specific geometry limits photon collection efficiency and overall enhancement. Model predictions indicate that 2-3% enhancement is realizable in DSSC minimodules, compared to minimodules using passive, non-luminescent, UV-BL. As the LSS DS films can be fabricated via low cost industrial chemical processes such as blending or grafting, they can be incorporated into production lines of DSSC technology in place of UV-BL typically used.

2. Experimental

2.1 $Eu(tta)_3phen$ complex synthesis

The $Eu(tta)_3phen$ complex (Figure 1) was prepared from $EuCl_3.6H_2O$ chloride. A proper amount of $EuCl_3.6H_2O$ was dissolved in methanol. A stoichiometric quantity of thenoyltrifluoroacetate ligand in methanol was added to the first solution. This solution was stirred for 30 minutes. The solution was kept at pH = 8 by adding NaOH saturated methanol solution, and was stirred for a further 30 minutes. A suitable amount of phenanthroline ligand was then added, and the $Eu(tta)_3phen$ precipitated. 30 minutes continuous stirring was carried out. Finally, the complex was recovered by using a Büchner funnel, and cleaning with methanol and drying in vacuum. The synthesis yield was 80%. The Europium based complex exhibits large Stokes shifted photoluminescence, absorbing in the UV region and emitting at "red" wavelengths. The luminescence process occurs in three steps: light absorption by the organic ligand, followed by highly efficient intraenergy conversion from the ligand singlet state to the triplet state by intersystem crossing, followed by energy transfer from ligand triplet state to the excited state of the lanthanide ion [22].

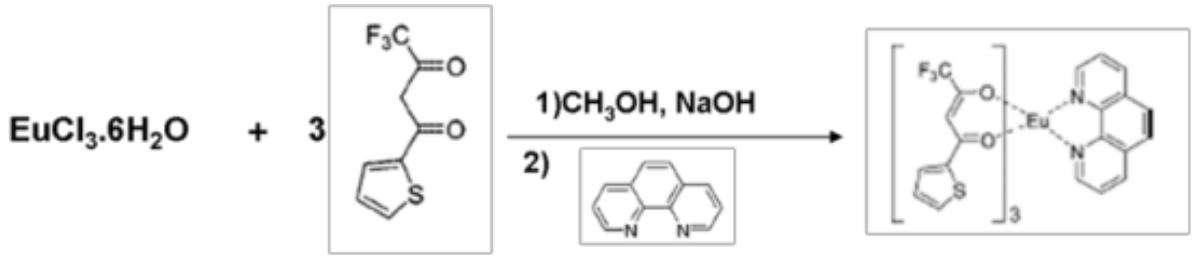

Figure 1. Synthesis of Eu(tta)$_3$phen complex.

Films containing lanthanide complex were prepared through a blending technique where the complex and the pure polymer are both dissolved in a cosolvent. Uniformly doped PVB (Butvar B-98, Solutia Inc.) films were prepared by drop casting in Teflon moulds on a levelled surface using tetrahydrofuran solvent. The absorption and PL spectra of Eu(tta)$_3$phen complex in PVB films are shown in Figure 2. The large Stokes shifted PL is evident. This is an important characteristic for DS layers as (a) optical transmission in visible wavelengths is maximised where DSSC EQE is high, and (b) "self-absorption" losses of DS-emitted photons in the layer are avoided if absorption and emission bands do not overlap. Absorbance was measured on a Perkin Elmer UV/VIS 900 spectrometer. PL spectra was measured on a Perkin Elmer LS55 fluorimeter fitted with Hamamatsu R6925 gated photomultiplier tube.

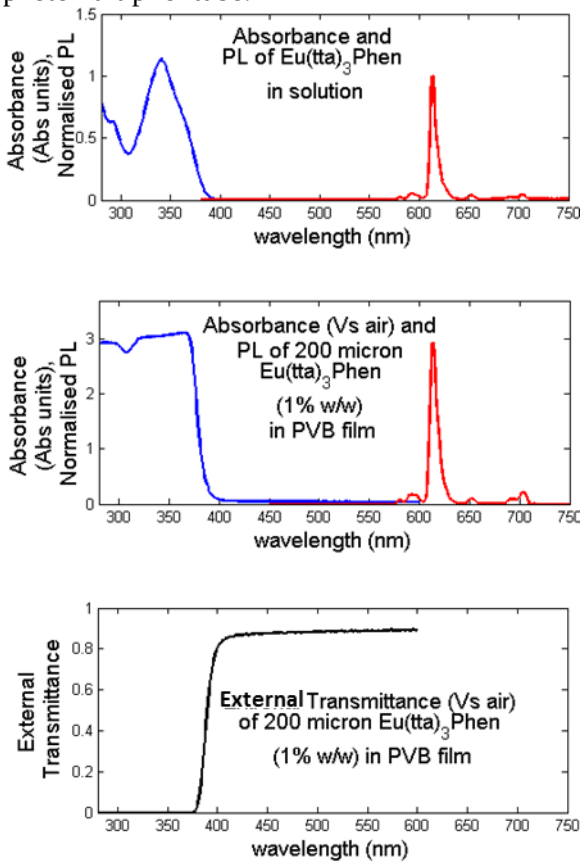

Figure 2 Absorption and photoluminescence spectra of Eu(tta)$_3$phen complex in solution (top) and in PVB film (centre). Also shown (bottom) is the external transmission of the Eu complex film.

2.2 Photoluminescent quantum yield (Φ) measurements in solid films

A high luminescent quantum yield, Φ, is required to maximize solar cell efficiency gains through a DS process. Quantified Φ of Eu(tta)$_3$phen in solid thin films though reported infrequently it has been shown to be dependent on the doping concentration and on the specific host medium

[23, 24, 25]. Φ is determined using an integrating sphere method [26,27,28], where the number of photons emitted is quantified relative to the total excitation photons absorbed by the sample. Monochromated excitation light at 360nm (FWHM ~10nm) is coupled into the integrating sphere via optical fibre. A CCD spectrometer (AVASPEC 2048-USB2) is used to monitor the photon count rate exiting at the measurement port of the integrating sphere. All measured emission spectra are corrected for the spectral response of the detector system in totality. The photon count rate is measured for three cases; a) sphere empty, b) sphere containing "test" sample film, c) sphere containing a "blank" polymer sample film with no active luminescent molecules, and measured using two excitation wavelengths; 1) within absorption range of the DS molecules, and 2) at longer wavelength within DS emission spectral range. Φ is given by;

$$\phi = \frac{\text{photons emitted}}{\text{photons absorbed}} = \frac{(\sum E_{s1})(\sum L_{n2}/\sum L_{s2})}{\sum L_{b1} - \sum L_{s1}}$$

where *E* and *L* are the corrected emission and excitation light spectra, respectively. The subscripts "s", "b", and "n" refer to whether the integrating sphere contains the sample, the blank, or is empty, respectively, and subscripts "1" and "2" refer to the two excitation wavelengths described above. The self-absorption correction technique used in solid film, integrating sphere, quantum yield measurements [27,28] is not required for the Europium complex as minimal self-absorption is present due to the LSS PL.

2.3 DSSC / LSS DS device fabrication

In fabrication of the DSSCs, TiO_2/FTO photo-electrodes and Pt/FTO counter-electrodes (DyeSol) are used. The photo-electrode is sensitized with N719 ($C_{58}H_{86}N_8O_8RuS_2$, DyeSol) dye, by dipping in N719 (0.5 mM ethanol solution 96% v/v de Scharlab) for approximately twelve hours. The photo-electrodes are cleaned to remove excess dye and dried with compressed air. The electrolyte used is 0.50M LiI (99,90% purity, Sigma-Aldrich), 0.050M I_2 (99,999% purity, Sigma-Aldrich), and 0.5M tert-butylpyridine, TBP, (96% purity, Sigma-Aldrich) in 3-metoxy-propionitrile (3MPN). A hole ~1.1 mm in diameter is drilled in the Pt/FTO counter-electrode, and afterwards the electrode is cleaned. The sensitized photo-electrode and the counter-electrode are mounted with a thermoplastic spacer (Surlyn 30, DyeSol) between them. A soft thermal process is carried out to seal the DSSC. The electrolyte is introduced via the counter electrode hole and the hole is sealed. A comparison is made between the electrical output of four types of devices, shown in Figure 3;

1: Bare N719 DSSC,
2: N719 DSSC + UV-BL (400 nm cutoff),
3: N719 DSSC + LSS DS layer,
4: N719 DSSC + UV-BL + LSS DS layer.

As the UV cut-off wavelength of the LSS DS layer (~390 nm) is slightly shorter than the UV-BL layer (400 nm), device 4 allows efficiency enhancement to be analysed independently from any favourable/biased transmission variation between the UV-BL and LSS DS layer.

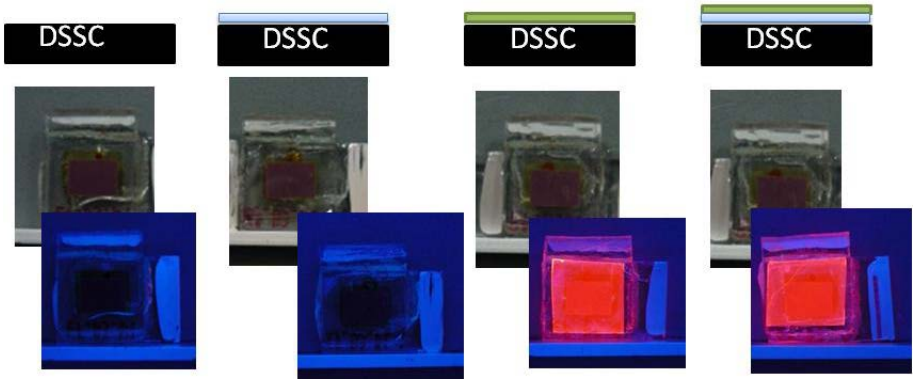

Figure 3: N719 DSSC devices. (From left to right) The bare DSSC device, DSSC + UV-BL, DSSC + LSS DS, and DSSC + UV-BL + LSS DS. Devices are photographed under daylight (top) and UV light (bottom).

2.4 Electrical characterisation:

EQE measurements are taken under bias lighting on a QEX10 Quantum Efficiency (PV Measurements Inc) with xenon arc lamp source. The monochromatic beam area is ~1 cm^2 and directed at the centre of the cell. The EQE measurements were performed over the wavelength range 300 nm to 1200 nm in steps of 10 nm. Three EQE values were obtained for each wavelength measured. The instrument repeatability is quoted from manufacturer as ±0.3% in the 400-1000 nm range and better than ±0.6% in the 300-400 nm and 1000-1200 nm ranges. As the DS layers attached cover an area slightly greater than the active area of the bare DSSC, samples are masked during electrical testing to ensure active area is equivalent in each case. Relative (or absolute) device short circuit current density (Jsc), under air-mass 1.5 spectral irradiance, can be calculated from the integrated product of EQE times the incident spectrum photon flux.

2.5 Accelerated ageing measurements of LSS DS layers

The photostability of the polymer LSS DS films is studied by applying a rigorous colour fastness test standard (UNE-ISO 105-B02 test). Tests are performed using a Xenotest accelerating ageing test chamber with Xenochrome 320 filter. Samples are exposed to 100 hour continuous irradiation (42 Wm^{-2} UV component) at a temperature of 50°C and relative humidity 40±5%. Colorimetry studies are performed prior to and after ageing. The colorimetry results are evaluated using the "colour difference parameter", ΔE, whereby a colour difference below 1 indicates that any change is not visually perceptive.

3. Ray-trace analysis

A 3-dimenional Monte-Carlo ray-trace modeling technique [29,30,31,32] is used to predict the photon flux emerging from the DS layer surfaces and the flux transmitted to the attached solar cell. From this, the modified EQE and Jsc of the DSSC/DS device is calculated. In the model, incident photons (of a given wavelength) are represented by ray vectors and traced through a device configuration until the ray reaches the PV cell, is emitted/reflected out of the device, or absorbed in the DS or glass layers. As each ray intersects a surface boundary, the probability of a reflection or transmission "event" is determined from the Fresnel reflection equations. A Monte-Carlo technique is used to determine which "event" occurs, (i.e. the calculated probability is tested against a randomly generated number in the interval [0,1]). The probability of an absorption event occurring between boundaries is calculated using the measured DS absorption spectrum and the Beer-Lambert law. The probability of an emission event is given by Φ. PL is assumed to isotropically distributed spatially, and non-polarised. The wavelength of an emitted photon/ray is assigned at random from a weighted spectral distribution corresponding to the measured PL spectrum of the DS material. Model output has been shown to compare well to measured optical and electrical output of luminescent solar concentrator PV devices [33], and to analytic [31], and other numerical models [33, 34] of luminescent layers.

If the DS absorbance spectrum and bare cell EQE overlap, the DS layer may decrease EQE at the overlapping wavelengths, depending on the specific DS efficiency and the EQE at absorption and emission wavelengths [17, 19]. The spectrally-resolved ray-trace model can be used to investigate the trade-off between maximising enhancement from the DS layer in the UV region, whilst minimising possible absorption losses at longer wavelengths where the DSSC EQE is higher. The model is used to optimise the thickness and concentration of the LSS DS layers for the specific DSSC, and to quantify the optical losses arising in small area, single-cell, DSSC devices.

4. Results and discussion

4.1 LSS DS film photoluminescent and photostability properties

Measured luminescent quantum yield, Φ, of the luminescent films is ~72% (shown in Table 1), and moreover, there is no significant variation in Φ with higher complex concentration up to 5% w/w. However, partial agglomeration and/or possible crystallisation of the complex is evident in the highest concentration film (5% w/w), as shown in Figure 4. The high concentration (5%) is, therefore, not considered for inclusion in DS layers. The complex was also tested in PMMA host polymer, with equivalent Φ. However, PMMA has a lower transmission at UV wavelengths and was found to be more brittle than PVB in the 200 micron thick films.

Table 1. Measured luminescent quantum yield, Φ, of lanthanide $Eu(tta)_3phen$ complex in PVB (Butvar 98B) polymer thin films. The colour difference parameter, ΔE, indicates the change in film colour after accelerated ageing tests.

Eu complex Conc. (w/w) %	**PL Quantum Yield, Φ**	**Colour difference, parameter ΔE**
0.1	0.67 ± 0.08	1.4
1.0	0.76 ± 0.08	8.7
5.0	0.76 ± 0.08	16.8

The stability of $Eu(tta)_3phen$ in the PVB films was studied using a standard accelerated ageing test described in section 2.5. Figure 4 shows the films prior to and after ageing tests. Following the 100-hour continuous UV irradiation, photoluminescence is not visible under UV light and the films exhibit a yellow tinge. The colour difference parameter in Table 1, which increases at higher Eu complex concentration, indicates that decomposition of the complex alters the film colour and reduces the overall transmission. The particular films do not exhibit sufficiently photostable to act as effective UV blockers and downshifters in medium-long term outdoor conditions. Fukuda et al. [24] have demonstrated, however, that encapsulating Eu complexes in sol-gel host media can greatly improve the long-term stability of the complex.

If the photostability can be improved, sections 4.2, 4.3, and 4.4 below demonstrate that significant performance enhancement in DSSCs can be realised using $Eu(tta)_3phen$ LSS DS.

0.1% $Eu(tta)_3phen$		1.0% $Eu(tta)_3phen$		5.0% $Eu(tta)_3phen$	
UV lamp	White light	UV lamp	White light	UV lamp	White light
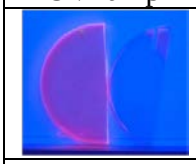	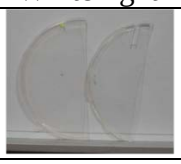			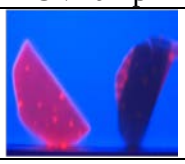	
Before /after	Before/after	Before /after	Before /after	Before /after	Before /after

Figure 4. $Eu(tta)_3phen$/PVB films before and after accelerated ageing tests. Photos are taken under UV light (left) to show PL, and under white light (right) to show visible change in colour. PL is destroyed in the aged films and they exhibit a yellow tinge post ageing.

4.2 Predicted LSS DS enhancement from varying film thickness and doping concentration.

The ray-trace model is used to calculate the enhancement in Jsc resulting from $Eu(tta)_3phen$ layers of varying concentration and thickness. The results in Figure 5B show that marginal enhancement in Jsc (<0.2%) is possible from addition of the LSS DS layer on the bare DSSC. Up to 2.7% enhancement in Jsc is predicted, relative to a DSSC with UV-BL. In this case, a LSS DS thickness of ~200 microns is optimal, if using 1% w/w concentration.

It is important to note that the DSSC glass top cover is not explicitly considered in the model, here in section 4.2, i.e. the thickness of the glass top cover is assumed to be negligible. In doing so, we calculate the maximum gains attainable from *spectrum modification* by an optimised DS layer,

independent from optical losses arising from low photon collection efficiency *small-area*, single-cell DSSCs. These optical losses shown to be dependent on the thickness of the glass to cover are analysed and discussed in section 4.4.

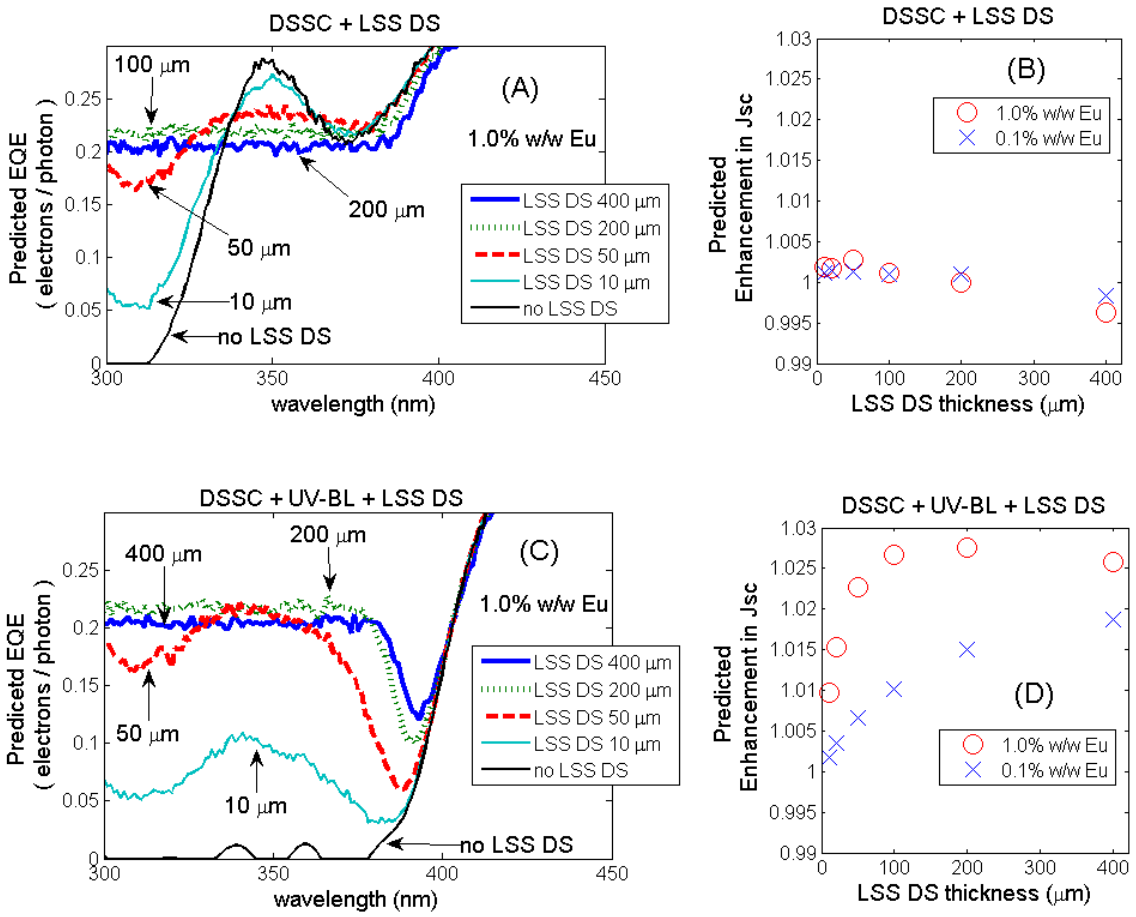

Figure 5. (A, C). Predicted EQE of (11mm x 8mm) N719 DSSC with LSS DS layers of varying thickness, using 1.0% Eu complex concentration (B,) The predicted *maximum* enhancement in Jsc is shown for varying LSS DS thickness assuming 0.1%, and 1.0% complex concentration. A bare N719 DSSC is considered in (A) and (B), and marginal enhancement in Jsc is predicted (<0.2%). A N719 DSSC+UV blocker device is considered in (C) and (D), where significant enhancement (2.7%) in Jsc is predicted using 1.0% w/w concentration, and 200 micron LSS DS film thickness.

The predicted Jsc enhancement in Figure 5D assumes a model input spectral irradiance corresponding to the ASTM Air Mass 1.5 *Global* solar spectral irradiance (AM1.5G). Gains from DS are highly dependent on the specific incident spectral irradiance [35, 36]. DS gains are higher in diffuse, conditions (where the solar irradiance has a high average photon energy, and a greater fraction of the spectrum is within the LSS DS absorption range). The predicted enhancement using Eu(tta)3phen assuming an approximate[i] *diffuse* solar spectral irradiance is 4.3%, compared to 2.7% under standard Am1.5G irradiance. Annual energy output enhancement, therefore, will be higher than the corresponding power conversion efficiency enhancement measured with AM1.5G.

4.3 Measured external quantum efficiency characterisation of DSSC + LSS DS devices

[i] calculated from the ASTM AM1.5 *Global* – ASTM AM1.5 *Direct* solar spectra

The measured EQE of the DSSC devices are presented in Figure 6. The UV-BL reduces the EQE in the UV region of the spectra, as expected. The LSS-DS layer also reduces EQE in the UV region relative to the *bare* DSSC. However, significant enhancement in EQE is attained from the LSS DS relative to the DSSC+UV-BL device. From the measured EQE, and assuming ASTM 1.5G incident spectral irradiance, we calculate that ~1% increase in DSSC Jsc will accrue due to *downshifting*.

Significant optical losses arise due to the specific geometry of the protoype DSSCs. Higher gains from the same LSS DS layers will result, if thinner glass cover layers can be utilized, and/or larger area DSSC minimodules are used, as discussed below in section 4.4.

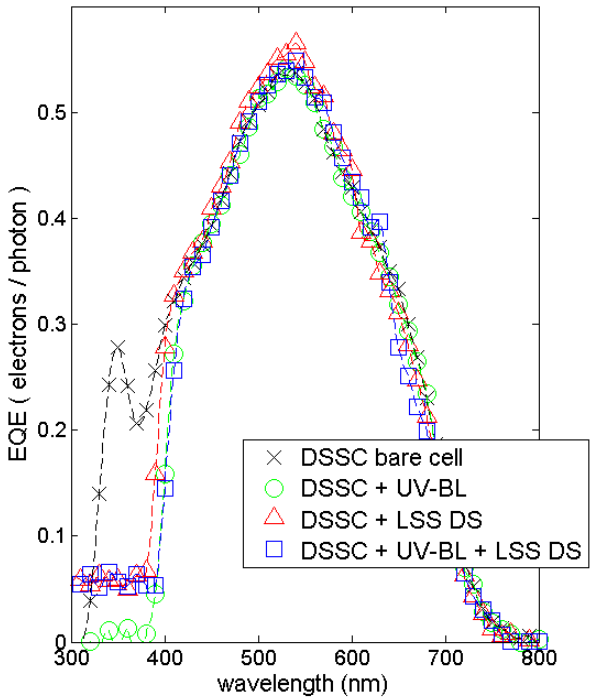

Figure 6. Measured EQE of N719 bare DSSC (x), with UV-BL (circles), with LSS DS (triangles), and with UV-BL+LSS DS layer (squares). Increase in EQE is demonstrated in devices with LSS DS, relative to DSSC+UV-BL.

4.4 Optical losses of DS-emitted photons in small area, single-cell, DSSCs

The measured EQE at UV wavelengths in the DSSC + UV-BL + LSS DS device (Figure 6) is lower than that predicted in Figure 5. In Figure 5, however, DSSC glass top cover is assumed to be negligible. In the actual single-cell DSSC devices fabricated, the 3mm thick cover glass significantly decreases the fraction of DS emitted photons transmitted to the photoactive layer in the DSSC, as illustrated in Figure 8(A). The DS photon collection efficiency is >80% in the 8 x 11 mm photoactive area devices, when the cover glass layer thickness approaches 0mm. With a cover glass layer thickness of 1mm or 3mm, the predicted collection efficiency is ~56% and ~40%, respectively. The predicted EQE for devices with thinner glass cover layers is shown in Figure 9. EQE enhancement from DS in small area DSSC cells can be improved by using a thinner glass. The optical losses and photon collection efficiency are specific to the particular dimensions of the DSSC device. If larger area DSSC minimodules are fabricated, neighbouring adjacent photoactive region collect the guided photons, thereby increasing DS collection efficiency, as illustrated in Figure 8(B). Secondary benefits of the LSS-DS layer on DSSC *minimodules* also accrue, as better use of made of the non photoactive area[ii].

[ii] In larger DSSC minimodules, "gap" regions with no photoactive material typically exist where the thermoplastic spacing/sealant is used. It is also noted that the LSS DS layers placed on top of the DSSC

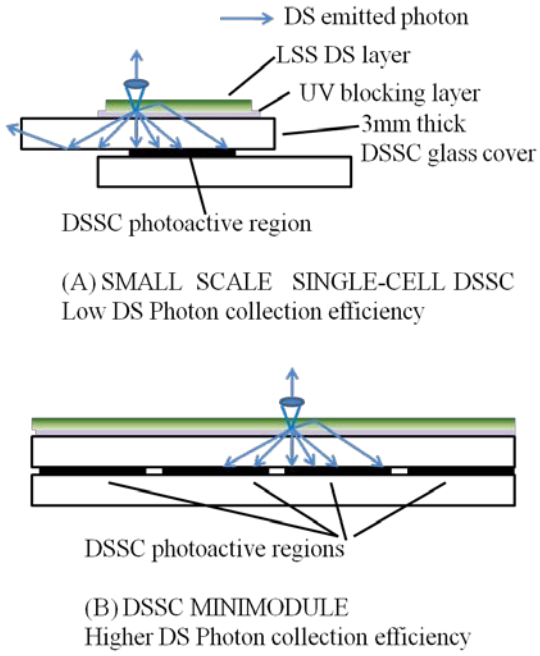

Figure 8. Schematic depicting sample paths of DS emitted photons. (A) In a single-cell prototype DSSC photoactive region is separated from the DS layer by the glass top cover. Significant optical losses arise, as DS-emitted photons are emitted away from the photoactive region. In this case, predicted DS collection efficiency is ~40%.. For (B) larger area DSSC minimodules, neighbouring adjacent photoactive regions collect "guided" photons, thereby increasing the DS collection efficiency and overall gain.

Collection efficiency increases as the top glass cover thickness is reduced see Figure 9. By reducing the glass thickness in small area single-cell DSSCs, predicted enhancement in EQE is increased as there is a higher DS photon collection efficiency. The predicted EQE of the single-cell DSSC device assuming the actual 3mm glass thickness (as shown in Figure 9) is still higher than the measured EQE of the equivalent device (Figure 6). Although no definitive explanation can be given, it could be due to some combination of (a) underestimation of the optical edge losses in the model compared to the fabricated device, (b) photon reflection at the multiple layer interfaces[iii] which is not considered in the model, (c) overestimated luminescent quantum yield, and/or (d) idealistic isotropic emission assumption in the model which has been shown to lead to underestimatation in escape-cone losses in luminescent layers [37].

minimodule can make better use of the "gap" space and further enhance the gains ensuing from the LSS DS layer.

[iii] i.e., LSS DS layer/adhesive, adhesive/UV-BL, UV-BL/adhesive, and adhesive/DSSC interfaces.

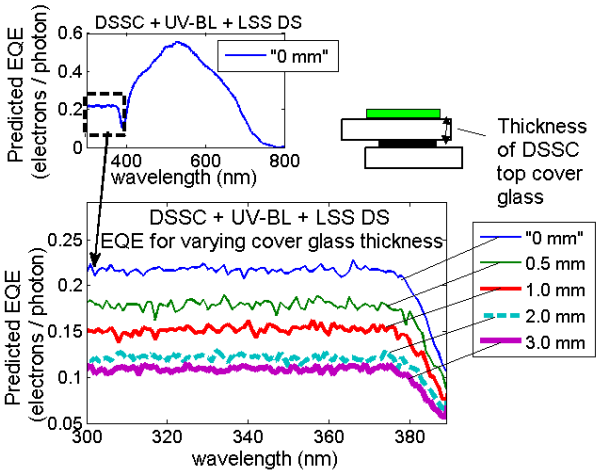

Figure 9. Predicted EQE of DSSC + UV-BL + LSS DS layer (1% $Eu(tta)_3phen$). The thickness of the actual DSSC glass layer is ~3mm (see Figure 8).

5. Summary and Conclusions

In current DSSC PV, ultraviolet blocking layers (UV-BL) avoid photocatalysis effects on the dye that reduces PV energy output over time. While the use of a UV-BL increases stability, power conversion efficiency decreases as incident UV photons are not converted. It is shown that large Stokes shift downshifting (LSS DS) layers can be used as a type of "active" UV blocking layer in DSSCs. The organolanthanide complex $Eu(tta)_3phen$ has been examined for inclusion in LSS DS layers. Polymer films were prepared and attached to DSSC devices. A ray-trace numerical model was used to optimise the thickness and concentration of the LSS DS layers for the specific N719 type DSSC. The 390 nm cutoff cut off wavelength of the $Eu(tta)_3phen$ film is analogous to passive UV-BL typically used in DSSCs. The EQE of DSSCwith LSS DS layer is significantly increased in the UV spectral region compared to DSSCs with a passive UV-BL. Previous studies using small Stokes shift DS dyes with DSSCs showed that EQE enhancements in the UV region were outweighed by losses in EQE from dye absorption at visible wavelengths. The high transparency of the *LSS* DS $Eu(tta)_3phen$ films in the visible range results in minimal EQE losses at visible wavelengths. Jsc is increased (by ~1%) relative to DSSCs utilizing "passive", non-luminescent UV-BL.

Optical losses of DS-emitted photons arise due to the specific geometry of small-area (~1cm^2) lab produced DSSCs. Ray-trace modelling shows how these optical losses can be reduced in prototype single-cell DSSCs by the use of a thinner glass top cover. These optical losses should become less significant in larger DSSC minimodules.

During a 100-hour continuous accelerated ageing test, photoluminescence is destroyed in the Eu complex LSS DS layers, and film discoloration is observed. The photostability of these particular blended films is not sufficient to be useful for medium-long term outdoor PV applications. However sol-gel encapsulation of the Eu complex has been shown to improve stability [24]. Significant DSSC performance enhancement is realizable from LSS DS layers, if photostable encapsulation of Eu complex layers can be thus realised. Approximately 1% gain in Jsc has been demonstrated in small scale DSSC prototypes. Model predictions indicate gains of 2-3% in DSSC minimodules are realizable, compared to DSSCs using passive UV-BL. Downshifitng gains from LSS DS layers can be over 50% higher in certain overcast, "diffuse" conditions compared to the gains measured using standard AM1.5G spectral irradiance. Therefore, the gains in daily DSSC minimodule *energy* yield from $Eu(tta)_3phen$ LSS DS could be 4-5%, depending on sky conditions.

Acknowledgements

The research is supported by the European Union as part of the Framework 7 integrated project EPHOCELL (227127)

References

Ahn, T.S., Al-Kaysi, R.O., Müller, A.M., Wentz, K.M., Bardeen, C.J. (2007) Self-absorption correction for solid-state photoluminescence quantum yields obtained from integrating sphere measurements, Rev. Sci. Instrum., 78 86105-1 -86105-3.

Alonso-Alvarez, D.; Ross, D.; McIntosh, K.R.; Richards, B.S.; (2012) "Performance of luminescence down shifting for CdTe solar cells as a function of the incident solar spectrum," *38th IEEE Photovoltaic Specialists Conference (PVSC), 2012*, 2504-2508, 3-8 June

Attia, M.S., Khalil, M.M.H., Abdel-Shafi, A.A., Attia, G.M., Failla, S., Consiglio, G., Finocchiaro, P., Abdel-Mottaleb, M.S.A. (2007) Factors Affecting the Efficiency of Excited-States Interactions of Complexes between Some Visible Light-Emitting Lanthanide Ions and Cyclophanes Containing Spirobiindanol Phosphonates, Int. J. Photoenergy, 1-7.

Binnemans, K. (2005) Rare-earth beta-diketonates, in: K.A. Gschneidner, Jr., J.C.G. Bünzli and V.K. Pecharsky (Eds.), Handbook on the Physics and Chemistry of Rare Earths Vol 35, Elsevier B.V., pp. 107-272.

Burgers, A.R., Slooff, L.H., Kinderman, R., Van Roosmalen, J.A.M. (2005) Modelling of Luminescent Concentrators by Ray-tracing. *Proceedings of 20th European Photovoltaic Solar Energy Conference*, Barcelona, Spain.

Carlos, L.D., Ferreira, R.AS., de Zea Bermudez, V., Ribero, S.J.L. (2009) Lanthanide-Containing Light-Emitting Organic-Inorganic Hybrids: A bet on the Future, Adv. Mater., 21, , 509-534.

Carrascosa, M., Unamuno, S., Agullo-Lopez, F. (1983) Monte-Carlo simulation of the performance of PMMA luminescent solar collectors. *Applied Optics,* 22, 3236-41.

Debije MG; Verbunt, PPE; Rowan BC; Richards BS and Hoeks TL. (2008) Measured surface loss from luminescent solar concentrator waveguides, Applied Optics, 47, 6763-6768.

De Mello, J. C., Wittmann F. H., and Friend, R. H. (1997) An improved experimental determination of external photoluminescence quantum efficiency, Advanced Materials, 9 230-232.

Fukuda, T., Yamauchi, S., Honda, Z., Kijima, N., Kamata, N. (2009) Improved stability of organic-inorganic composite emitting film with sol-gel glass encapsulated Eu-complex, Opt. Mater., 32, 207-211.

Gao, F., Wang, Y., Shi, D., Zhang, J., Wang, M., Jing, X., Humphry-Baker, R., Wang, P. ,Zakeeruddin, S. M., Grätzel, M. (2008) Enhance the Optical Absorptivity of Nanocrystalline TiO2 Film with High Molar Extinction Coefficient Ruthenium Sensitizers for High Performance Dye-Sensitized Solar Cells, J. AM. CHEM. SOC. 130, , 10720-10728.

Green, M. A., Emery, K., Hishikawa, Y., Warta, W., Dunlop, E. D. (2012) Solar cell efficiency tables (version 40), Prog. Photovolt: Res. Appl., 20, 606–614.

Hodgson, S.D., Brooks, W.S.M., Clayton, A.J., Kartopu, G., Barrioz, V., Irvine, S.J.C., (2013) Enhancing blue photoresponse in CdTe photovoltaics by luminescent down-shifting using semiconductor quantum dot/PMMA films. Nano Energy 2, 21-27.

Hovel, H.J., Hodgson, R.T., Woodall, J.M. (1979) The effect of fluorescent wavelength shifting on solar cell spectral response, Sol. Energy Mater., 2, 19-29.

Huang, X., Han, S., Huang, W., Liu, X. (2013) Enhancing solar cell efficiency: the search for luminescent materials as spectral converters, *Chem. Soc. Rev.,* 42, 173-201.

Kato, N., Higuchi, K., Tanaka, H., Nakajima, J., Sano, T., Toyoda, T. (2011) Improvement in long-term stability of dye-sensitized solar cell for outdoor use, Solar Energy Materials & Solar Cells, 95, , 301–305.

Kennedy, M., Rowan, B.C., McCormack, S.J., Doran, J., Norton, B. (2007) Modelling of a Quantum Dot Solar Concentrator and Comparison with Fabricated Devices, *Proceedings of 3rd Photovoltaic Science Application and Technology Conference*, Durham, UK.

Kennedy, M., Chatten, A.J., Farrell, D.J., Bose, R., Büchtemann, A., McCormack, S.J., Doran, J., Barnham, K.W.J., Norton, B., (2008). Luminescent Solar Concentrators: A Comparison of Thermodynamic Modelling and Ray-trace Modelling Predictions. *Proceedings of 23rd European Photovoltaic Solar Energy Conference and Exhibition*, Valencia, Spain, 334-7.

Klampaftis, E., Ross, D., McIntosh, K. R., Richards, B. S. (2009) Enhancing the performance of solar cells via luminescent down-shifting of the incident spectrum: A review, Sol. Energy Mater. Sol. Cells., 93, 1182-1194.

Kuang, D., Comte, P., Zakeeruddin, S. M., Hagberg, D. P., Karlsson, K. M., Sun, L., Nazeeruddin, Md., Grätzel, K., Stable M. (2011) Dye-Sensitized Solar Cells Based on Organic Chromophores and Ionic Liquid Electrolyte, Solar Energy, 85, 1189–1194

Le Donne, A., Acciarri, M., Narducci, D., Marchionna, S., Binetti, S. (2009) Encapsulating Eu3+ complex doped layers to improve Si-based solar cell efficiency, Progress in Photovoltaics, 17, 519–525.

Le Donne, A., Dilda, M., Crippa, M., Acciarri, M., Binetti, S. (2011) Rare earth organic complexes as down-shifters to improve Si-based solar cell efficiency, Opt. Mater., 33, 1012-1014.

Li, Q., Lin., J., Wu, J., Lan, Z., Wang, Y. Peng, F. Huang, M. (2013) Improving photovoltaic performance of dye-sensitized solar cell by downshift luminescence and p-doping effect of Gd_2O_3:Sm^{3+}, Journal of Luminescence, 134, , 59-62.

Liu, J., Yao, Q., Li, Y. (2006) Effects of downconversion luminescent film in dye-sensitized solar cells, APPLIED PHYSICS LETTERS, 88, 17, 173119- 1-3.

Marchionna, S., Meinardi, F., Acciarri, M., Binetti, S., Papagni, A., Pizzini, S., Malatesta, V., Tubino, R. (2006) Photovoltaic quantum efficiency enhancement by light harvesting of organo-lanthanide complexes, J. Lumin., 118, 325-329.

Maruyama, T., Kitamura, R. (2001) Transformations of the wavelength of the light incident upon CdS/CdTe solar cells, Sol. Energy Mater. Sol. Cells, 69, 61-8.

Nazeeruddin, M. K., Baranoff, E., Grätzel, M. (2011) Dye-sensitized solar cells: A brief overview, Solar Energy, 85, 1172–1178.

O'Regan, B. Grätzel, M. (1991) A low-cost, high-efficiency solar cell based on dye-sensitized colloidal TiO2 films, Nature, 353, 737-740.

Richards, B.S. (2006) Luminescent layers for enhanced silicon solar cell performance: Down-conversion, Solar Energy Materials & Solar Cells, 90, 9, 1189–1207.

Richards, B.S., McIntosh, K.R. (2007) Overcoming the poor short-wavelength spectral response of CdS/CdTe photovoltaic modules via luminescence down-shifting - ray-trace simulations, Progress in Photovoltaics, 15, 27-34.

Ross, D. Klampaftis, E., Fritsche, J., Bauer M. and Richards, B. S. (2012) Increased short-circuit current density of production line CdTe mini-module through luminescent down-shifting, Solar Energy Materials & Solar Cells, 103, 11-16.

Slooff, L. H., Kinderman, R., Burgers, A. R., Bakker, N. J., van Roosmalen, J. A. M. , Büchtemann, A., Danz, R., Schleusener, M. (2007) Efficiency Enhancement of Solar Cells by Application of a Polymer Coating Containing a Luminescent Dye, Journal of Solar Energy Engineering, 129, 3, 272-276.

van Sark, W.G.J.H.M. (2008) Simulating performance of solar cells with spectral downshifting layers, Thin Solid Films 516 6808–6812,

van Sark, W.G.J.H.M., Meijerink, A., Schropp, R.E.I., van Roosmalen, J.A.M,. Lysen, E.H. (2005) Enhancing solar cell efficiency by using spectral converters, Sol. Energy Mater. Sol. Cells, 87, 395-409.

van Sark, W.G.J.H.M., Barnham, K.W.J., Slooff, L.H., Büchtemann, A., Meyer, A., McLafferty, J.B., Koole, R., Chatten, A.J., Farrell, D.J., Bose, R., Bende, E.E., Quilitz, J., Kennedy, M., Meyer, T., Wadman, S.H., Meijerink, A., Vanmaekelbergh, D. (2008) Luminescent Solar Concentrators - A review of recent results. *Optics Express*, 16, , 21773-21792.

Wilson, L. R., Richards, B. S. (2009) Measurement method for photoluminescent quantum yields of fluorescent organic dyes in polymethyl methacrylate for luminescent solar concentrators, Applied Optics, 48, 212-220.